

Electronic Supplementary Information (ESI)

Synchronously improved luminescent efficiency and thermal stability of organic-inorganic chloride single crystals through doping of Sb³⁺

Zongqi Chen,^a Aibo Li,^a Yushan Xie,^a Haoqi Long, Qiang Zhou, ^{*a} Long Jiang^b, Peng Ren,^a and Zhengliang Wang,^{*a}

^{a)} Key Laboratory of Green-chemistry Materials in University of Yunnan Province, Yunnan Key Laboratory of Chiral Functional Substance Research and Application, School of Chemistry & Environment, Yunnan Minzu University, Kunming, 650500, China.

^{b)} Instrumental Analysis & Research Center, Sun Yat-Sen (Zhongshan) University, Guangzhou, 510275, China.

Email: wzhl@ymu.edu.cn (Z. Wang)

q-zhou@ymu.edu.cn (Q. Zhou)

Experimental section

(1) Materials

All reagents and solvents including C₄H₁₂NCl (99.9%, Aladdin), MnCl₂•4H₂O (99.9%, Aladdin), Sb₂O₃ (99.9%, Aladdin), HCl aqueous solution (37%, Aladdin), and ethanol (99.5%, Aladdin) were used without further purification. YAG:Ce³⁺ phosphors were purchased from Shenzhen Quanjing Photon Co. Ltd.

(2) Synthesis of (CH₃)₄NMnCl₃:xSb³⁺ (x = 0, 0. 2%, 0. 5%, and 1%) single crystals

Taking the preparation of (CH₃)₄NMnCl₃:0.5%Sb³⁺ as an example, 2 mmol MnCl₂•4H₂O and 0.005 mmol Sb₂O₃ were dissolved in 5 mL of HCl (36 wt %) solution at room temperature to form a transparent precursor solution. Then, 2 mmol C₄H₁₂NCl was added to the precursor solution with stirring for 4 h. Pink (CH₃)₄NMnCl₃:0.5%Sb³⁺ rod crystals grew up from this solution after one week at room temperature.

(3) Characterization

Single-crystal X-ray diffraction of(CH₃)₄NMnCl₃ crystals were selected and on a SuperNova AtlasS2 diffractometer (Rigaku Oxford Diffraction). Data was collected with Cu K α or Mo K α radiation at 293 K, respectively. Using Olex2, the structure was solved with the ShelXT structure solution program using Intrinsic Phasing and refined with the ShelXL refinement package using Least Squares minimization. All non-hydrogen atoms were located in different Fourier syntheses and finally refined with anisotropic displacement parameters. All hydrogen atoms of the organic ligands were

placed by geometrical considerations and isotropically refined with fixed U values using a riding model. The phase and crystal structure of the phosphors were determined by a Bruker D8 Advance powder X-ray diffraction (Cu K α radiation, $\lambda = 0.15406 \text{ \AA}$, 40 kV, 40 mA). Their morphology and element composition were characterized by a scanning electron microscope (SEM, FEI Quanta 200) with an accompanying energy-dispersive X-ray spectroscopy (EDS). To obtain high quality SEM images, the samples should be uniformly dispersed on the silicon wafer and sprayed with gold. The excitation (PLE) and emission (PL) spectra at different temperatures were measured by a fluorescence spectrometer (Hitachi F-7000). The fluorescence decay curves were measured using an FLS1000 steady-state fluorescence spectrometer. The diffuse reflectance ultraviolet-visible (DRS) spectra were tested using a UV-Vis spectrophotometer (UV-2550, Shimadzu, Japan).

(4) Fabrication of the white LED

The warm white LEDs were fabricated by coating $(\text{CH}_3)_4\text{NMnCl}_3:x\text{Sb}^{3+}$ with YAG:Ce $^{3+}$ commercial 460 nm LED chips. The luminescence of the white LED in the current range from 20 to 300 mA was detected on a highly accurate array spectrometer (HSP 6000).

Figures

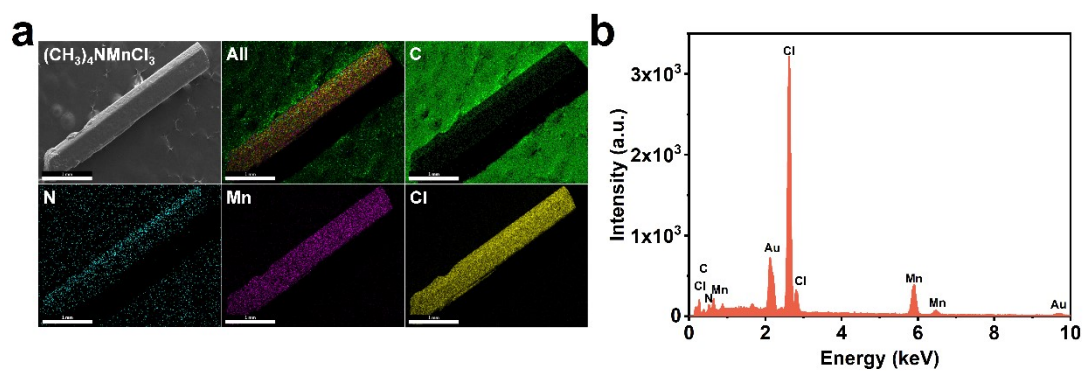


Fig. S1 Elemental mapping images and EDS curve of $(\text{CH}_3)_4\text{NMnCl}_3$.

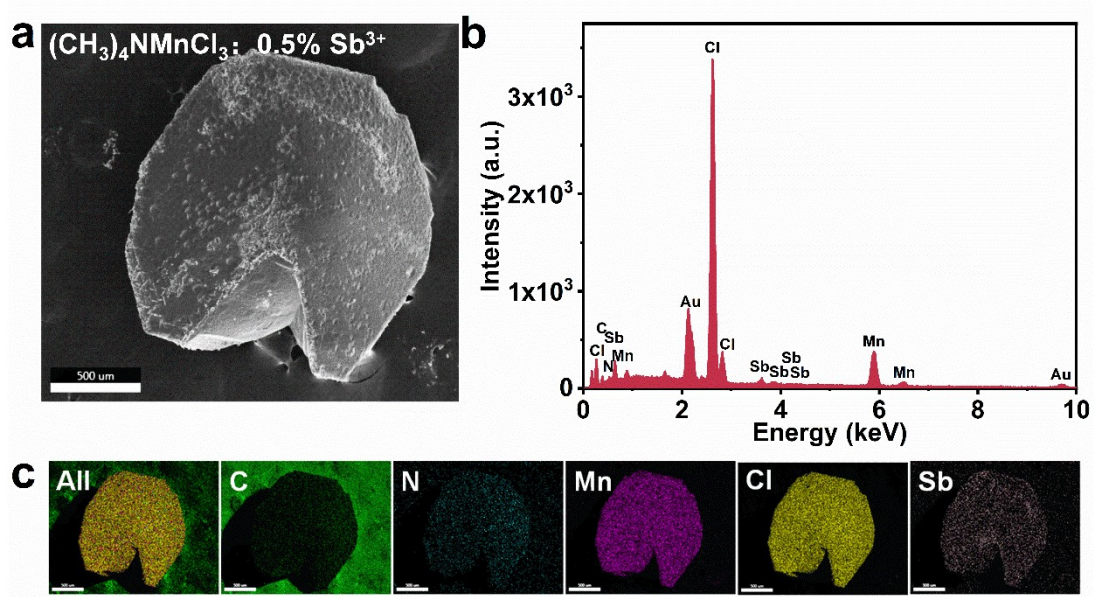


Fig. S2 Elemental mapping images and EDS curve of $(\text{CH}_3)_4\text{NMnCl}_3$:0.5% Sb^{3+} .

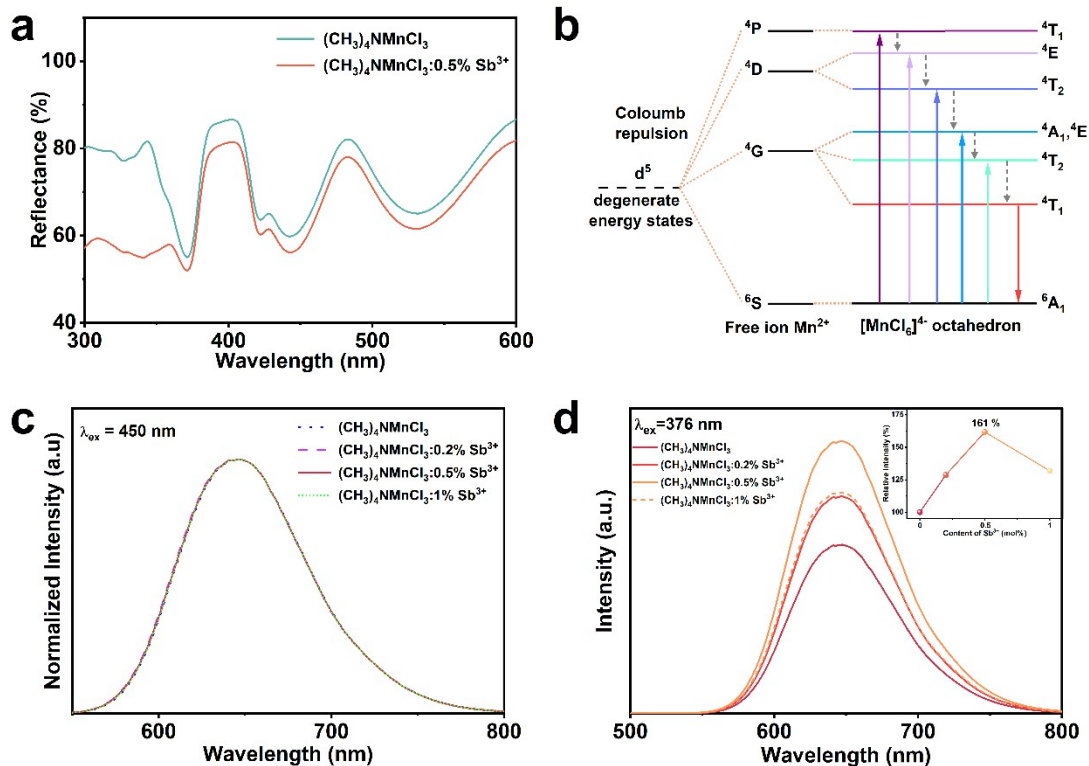


Fig. S3 (a) DR spectra of $(\text{CH}_3)_4\text{NMnCl}_3$ and $(\text{CH}_3)_4\text{NMnCl}_3:0.5\%\text{Sb}^{3+}$, (b) The schematic diagram showing the energy absorption, non-radiative relaxation, and radiative transition processes of Mn²⁺ in $(\text{CH}_3)_4\text{NMnCl}_3$; (c) PL spectra of $(\text{CH}_3)_4\text{NMnCl}_3:x\text{Sb}^{3+}$ under 376 nm excitation; (d) Normalized PL spectra of $(\text{CH}_3)_4\text{NMnCl}_3:x\text{Sb}^{3+}$ under 450 nm excitation.

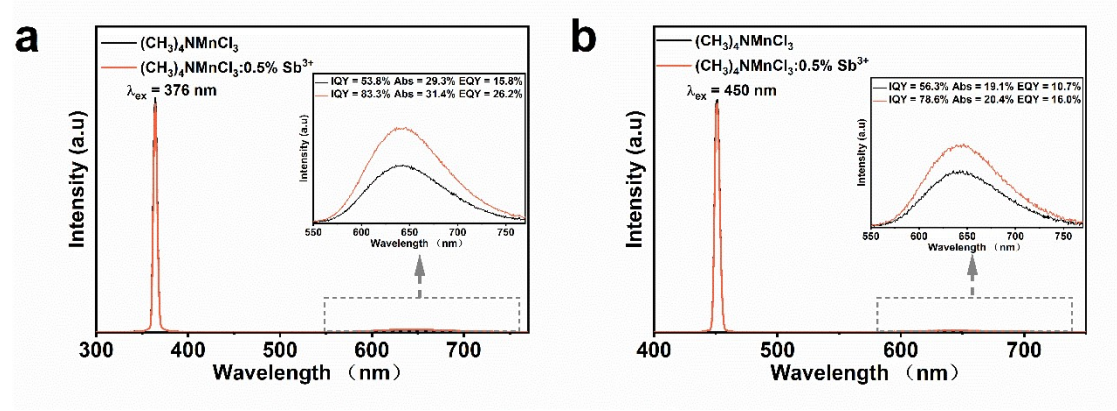


Fig. S4 PLQY plots of (CH₃)₄NMnCl₃ and (CH₃)₄NMnCl₃:0.5%Sb³⁺ crystals (a, $\lambda_{\text{ex}} = 376 \text{ nm}$; b, $\lambda_{\text{ex}} = 450 \text{ nm}$).

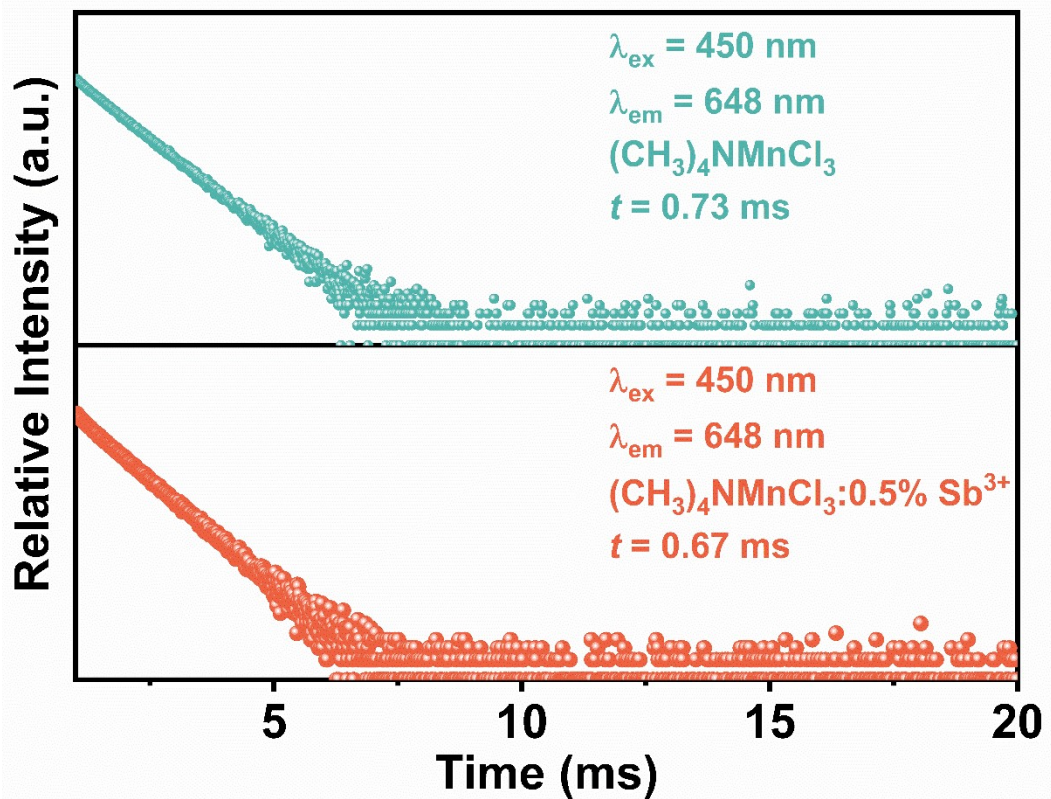


Fig. S5 PL decay curves of $(\text{CH}_3)_4\text{NMnCl}_3$ and $(\text{CH}_3)_4\text{NMnCl}_3:0.5\% \text{Sb}^{3+}$ crystals ($\lambda_{\text{ex}} = 450 \text{ nm}$, $\lambda_{\text{em}} = 648 \text{ nm}$).

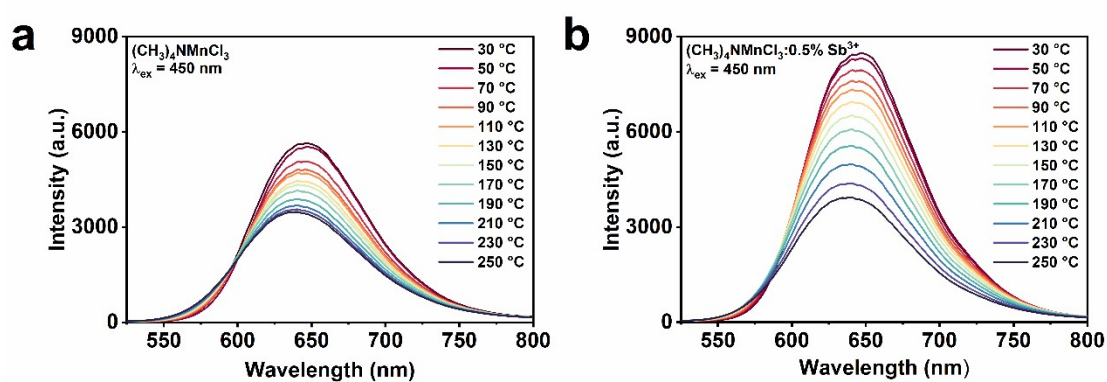


Fig. S6 Temperature-dependent emission spectra of (a) $(\text{CH}_3)_4\text{NMnCl}_3$ and (b) $(\text{CH}_3)_4\text{NMnCl}_3:0.5\%\text{Sb}^{3+}$

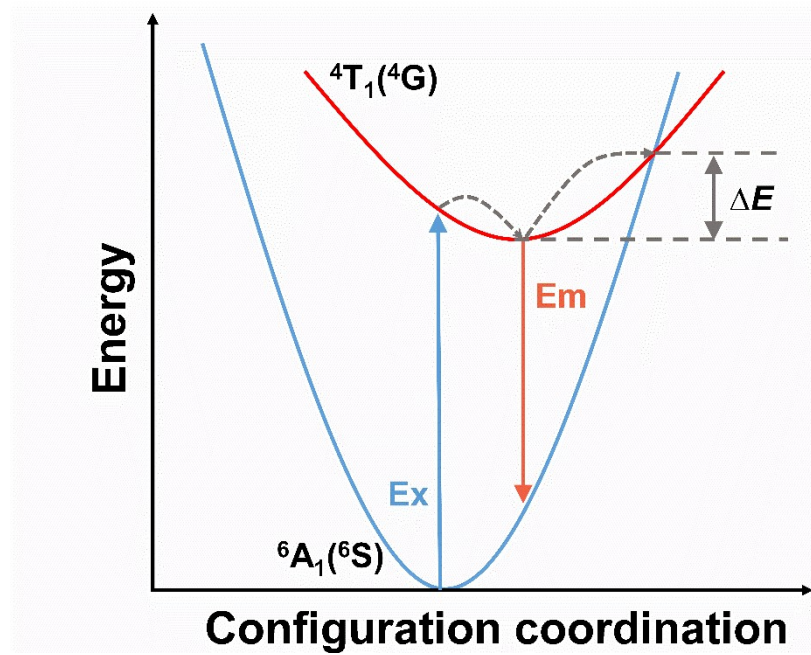


Fig. S7 Configurational coordination diagram showing the thermal quenching of Mn^{2+} emission

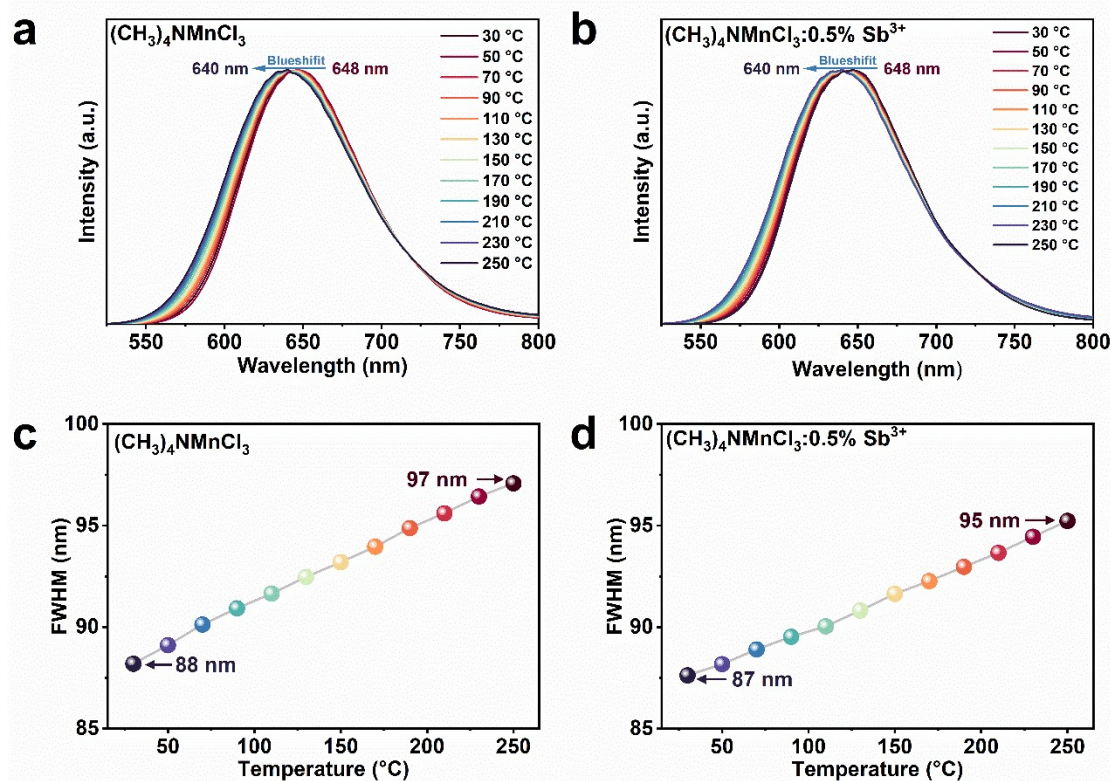


Fig. S8 (a, b) Normalized Temperature-dependent emission spectra of $(\text{CH}_3)_4\text{NMnCl}_3$ and $(\text{CH}_3)_4\text{NMnCl}_3:0.5\%\text{Sb}^{3+}$; (c, d) Plots of FWHM as a function of temperature.

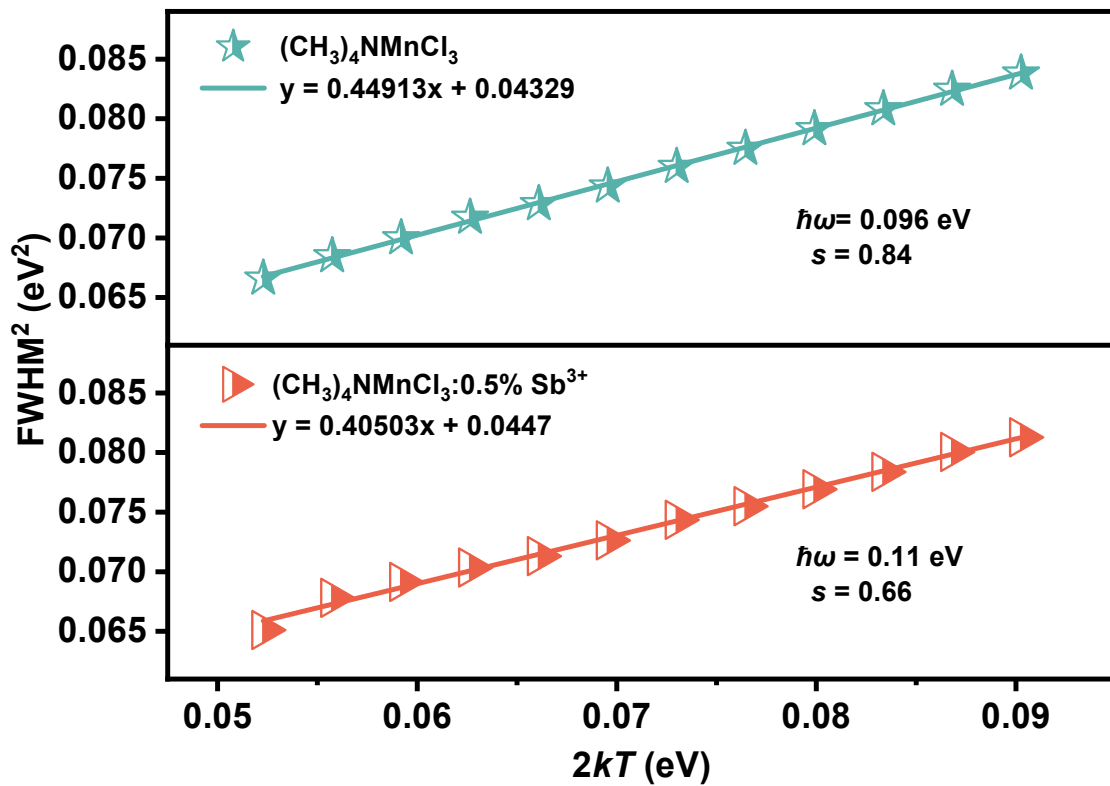


Fig. S9 Plots of FWHM 2 as a function of $2kT$

Table S1. Crystal structure parameters of $(\text{CH}_3)_4\text{NMnCl}_3$.

Formula	$(\text{CH}_3)_4\text{NMnCl}_3$
Temperature (K)	293
M_r	235.44
Crystal system	hexagonal
Space group	$\text{P}6_3/\text{m}$
a (Å)	9.1513
b (Å)	9.1513
c (Å)	6.4962
α (deg)	90
β (deg)	90
γ (deg)	120
V (Å ³)	471.15
Z	2
ρ_{calc} (g cm ⁻³)	1.660
μ/mm^{-1}	18.619
$F(000)$	238.0
Crystal size/mm ³	0.15 × 0.04 × 0.03
Radiation	CuK α ($\lambda = 1.54184$)
2 θ range for data collection/°	11.164 to 145.228
Index ranges	-11 ≤ h ≤ 10, -11 ≤ k ≤ 11, -8 ≤ l ≤ 7
Reflections collected	2776
Independent reflections	338 [$R_{\text{int}} = 0.0493$, $R_{\text{sigma}} = 0.0199$]
Data/restraints/parameters	338/73/58
GOF on F^2	1.106
R_1 [$I > 2\sigma(I)$]	$R_I = 0.0391$, $wR_2 = 0.0933$
wR_2 (all data)	$R_I = 0.0413$, $wR_2 = 0.0974$

Table S2. Fractional Atomic Coordinates ($\times 10^4$) and Equivalent Isotropic Displacement Parameters ($\text{\AA}^2 \times 10^3$) for $\text{C}_4\text{H}_{12}\text{Cl}_3\text{MnN}$. U_{eq} is defined as 1/3 of the trace of the orthogonalised U_{IJ} tensor.

Atom	x	y	z	$U(eq)$
Mn 1	0	1000	1000	30.6(4)
Cl 1	982.6(11)	8501.2(10)	7500	38.3(4)
N 1	3270(30)	6650(20)	2500(20)	35.1(14)
C 1	3600(30)	5250(30)	2930(60)	54(7)
C 2	4310(30)	8090(30)	3880(30)	64(6)
C 3	1470(30)	6060(30)	2900(60)	55(8)
C 4	3680(50)	7180(30)	330(20)	78(8)

Table S3. Anisotropic Displacement Parameters ($\text{\AA}^2 \times 10^3$) for $(\text{CH}_3)_4\text{NMnCl}_3$. The Anisotropic displacement factor exponent takes the form: -
 $2\pi^2[h^2a^*{}^2U_{11}+2hka^*b^*U_{12}+\dots]$.

Atom	U_{11}	U_{22}	U_{33}	U_{23}	U_{13}	U_{12}
Mn 1	34.7(4)	34.7(4)	22.4(6)	0	0	17.4(2)
Cl 1	49.6(5)	43.8(5)	31.7(6)	0	0	31.0(4)
N 1	35(7)	38(6)	40(3)	1(8)	3(8)	24(6)
C 1	62(9)	55(10)	52(15)	8(10)	19(9)	35(7)
C 2	60(11)	57(10)	54(10)	-18(9)	-1(9)	13(9)
C 3	26(8)	78(12)	49(16)	-13(10)	8(9)	16(7)
C 4	77(13)	70(13)	61(9)	25(9)	3(12)	17(9)

Table S4. Selected bond lengths and bond angles of $(\text{CH}_3)_4\text{NMnCl}_3$.

Bond	Length (Å)	Bond	Angle (°)
Mn 1-Cl 1¹	2.5614(6)	Cl 1¹-Mn 1-Cl 1²	180.0
Mn 1-Cl 1²	2.5614(6)	Cl 1³-Mn 1-Cl 1⁴	180.0
Mn 1-Cl 1³	2.5614(6)	Cl 1¹-Mn 1-Cl 1⁴	84.086(15)
Mn 1-Cl 1	2.5614(6)	Cl 1⁵-Mn 1-Cl 1⁴	84.086(15)
Mn 1-Cl 1⁴	2.5614(6)	Cl 1⁵-Mn 1-Cl 1³	95.914(15)
Mn 1-Cl 1⁵	2.5614(6)	Cl 1³-Mn 1-Cl 1	84.086(15)
N 1-C 1	1.476(10)	Cl 1¹-Mn 1-Cl 1³	95.914(15)
N 1-C 4	1.478(10)	Cl 1¹-Mn 1-Cl 1⁵	84.086(15)
N 1-C 3	1.482(10)	Cl 1²-Mn 1-Cl 1³	84.086(15)
N 1-C 2	1.477(11)	Cl 1²-Mn 1-Cl 1	84.086(15)
		Cl 1⁴-Mn 1-Cl 1	95.914(15)
		Cl 1²-Mn 1-Cl 1⁵	95.914(15)
		Cl 1¹-Mn 1-Cl 1¹	95.914(15)
		Cl 1²-Mn 1-Cl 1⁴	95.914(15)
		Cl 1⁵-Mn 1-Cl 1	180.0
Mn 1-Cl 1-Mn 1⁶	78.70(2)		
C 1-N 1-C 4		110.1(11)	
C 1-N 1-C 3		108.6(11)	
C 1-N 1-C 2		109.8(11)	
C 4-N 1-C 3		109.7(11)	
C 2-N 1-C 4		109.9(11)	
C 2-N 1-C 3		108.8(11)	

Table S5. Photoelectric parameters of white LED at different currents.

Phosphor	Current	LE	CIE		CRI	CCT	LF
	mA	lm/W	x	y		(K)	mW
YAG:Ce ³⁺ + <chem>(CH3)4NMnCl3</chem>	20	98.71	0.3721	0.3426	85.4	3970	17.5
	40	85.61	0.3715	0.3397	86.3	3964	33.4
	60	71.21	0.3717	0.3385	86.7	3957	42.8
	80	71.71	0.3701	0.3358	87.1	3974	61.3
	100	60.81	0.3696	0.3346	87.3	3978	67.2
	120	61.81	0.3682	0.3330	87.5	4014	81.8
	140	58.51	0.3673	0.3319	87.6	4034	94.3
	160	55.41	0.3664	0.3312	87.7	4065	103.3
	180	52.61	0.3659	0.3310	87.8	4078	111.4
	200	48.91	0.3666	0.3327	87.8	4069	117.3
	220	45.21	0.3660	0.3332	87.7	4092	121.3
	240	42.31	0.3636	0.3314	87.9	4167	126.3

Table S6. Photoelectric parameters of white LED-Sb different currents.

Phosphor	Current	LE	CIE		CRI	CCT	LF
	mA	lm/W	x	y		(K)	mW
	20	107.70	0.3794	0.3528	85.4	3831	18.1
	40	97.60	0.3783	0.3512	85.4	3855	36.2
	60	93.41	0.3773	0.3499	85.2	3872	53.6
	80	84.91	0.3777	0.3507	85.0	3867	62.7
YAG:Ce ³⁺	100	87.71	0.3755	0.3478	85.0	3910	85.8
+	120	77.71	0.3761	0.3483	84.2	3891	89.7
(CH ₃) ₄ NMnCl ₃ :	140	76.01	0.3743	0.3469	84.7	3934	109.3
0.5%Sb ³⁺	160	76.71	0.3731	0.3457	84.8	3966	129.6
	180	70.01	0.3720	0.3451	84.8	3992	142.0
	200	69.21	0.3711	0.3444	84.8	4020	154.6
	220	68.51	0.3706	0.3440	84.8	4030	167.0
	240	61.71	0.3698	0.3436	84.9	4058	175.7